2022-01-0437 Published 29 Mar 2022



# Spark Discharge Characteristics for Varying Spark Plug Geometries and Gas Compositions

Corey Tambasco, Matthew Hall, and Ronald Matthews The University of Texas at Austin

*Citation:* Tambasco, C., Hall, M., and Matthews, R., "Spark Discharge Characteristics for Varying Spark Plug Geometries and Gas Compositions," SAE Technical Paper 2022-01-0437, 2022, doi:10.4271/2022-01-0437.

Received: 20 Jan 2022 Revised: 20 Jan 2022 Accepted: 16 Jan 2022

## **Abstract**

park discharge properties were studied and characterized for varying gas compositions and spark plug geometries using a spark calorimeter and constant volume optical vessel. Two different 18 mm natural gas engine spark plugs were used in the experiments. All measurements were recorded under quiescent conditions and with a spark gap of 0.30 mm. The spark plug calorimeter was used for measuring thermal energy deposition to the gas for gas compositions of nitrogen, a stoichiometric mixture of nitrogen and methane, a stoichiometric mixture of nitrogen and methane diluted with 30% carbon dioxide by volume, and for air. Other measurements of interest included breakdown voltage, electrical energy delivered to the spark gap, electrical-to-thermal energy conversion

efficiency, and spark duration, for pressures up to 28 bar at 300 K. The optical vessel was used for the combusting mixture of stoichiometric air and methane at pressures up to 28 bar. For these combusting experiments, thermal energy deposition was unable to be measured. All measurements were performed on both an 18 mm natural gas engine spark plug with a J-shaped ground strap and an 18 mm natural gas engine spark plug with four individual ground straps, uniformly distributed around the plug's center electrode. Experiments showed consistently higher thermal energy deposition and electrical-to-thermal energy conversion efficiency for the J-shaped plug compared to the four-ground strap plug. Experiments also showed significant increases in breakdown voltage for air compared to nitrogen or nitrogen-based mixtures.

# Introduction

ewer spark ignition engines, and natural gas engines in particular, are being designed to run under increasingly challenging environments for emissions and efficiency purposes. This includes increased levels of boost pressure and leaner operating conditions. Under these circumstances, a significant increase in ignition energy is required for successful and reliable ignition from cycle-to-cycle with the use of conventional spark plugs [1]. This has motivated research to better understand the spark ignition process to improve ignition models and to develop spark plugs better suited for a long operational life.

A significant amount of previous research has been conducted looking at breakdown voltage trends and correlations. Many of those studies have been summarized in Meeks [2], presenting the increasing relationship of breakdown voltage with the product of pressure and spark gap distance as described by Paschen's Law. Pashley et al. [3] developed a new correlation for the breakdown voltage in air as a function of temperature, pressure, and gap distance. However, that study only looked at pressures up to 12 bar. Huang et al. [4] looked at pressures up to 40 bar and showed that the rate of increase in breakdown voltage begins to decline at pressures

above 12 bar, a failure of Paschen's Law. From this, they developed their own correlation for breakdown voltage as a function of the same variables. They also showed a slight increase in breakdown voltage in air when compared with nitrogen but showed negligible change in breakdown voltage in a nitrogenmethane mixture in comparison to just nitrogen. However, they did not consider combustible compositions.

Early studies of spark calorimetry were done by Roth et. al. [5] when they looked at the rate of heat loss from the energy delivered from a spark into its surrounding medium. They did this by measuring either the change in volume or the change in pressure from a constant pressure or constant volume chamber, respectively. Another early study was done by Teets et. al. [6] where they used a pressure-rise calorimeter to look at thermal energy deposition characteristics and electrical-to-thermal conversion efficiencies for three different spark ignition systems at pressures up to 7 bar. They found increases in both energy deposition and conversion efficiency with increasing pressure and spark plug gap size.

More recently, Abidin et. al. [7] used spark calorimetry to look at breakdown voltage and electrical-to-thermal energy conversion efficiencies whilst varying the parameters of pressure, spark plug gap, and dwell time. Their study found

an increase in energy conversion with increasing pressure, increasing spark plug gap length, and decreasing dwell time. However, they only considered pressures up to 9 bar in air. Franke et. al. [8] also used a spark calorimeter for measuring thermal energy deposition to the gas for multiple ignition systems and at pressures up to 16 bar. They found that electrical-to-thermal energy conversion efficiencies increased from 5% to around 50% at maximum pressure. They also found that efficiency increased with an increase in spark duration for a given delivered electrical energy.

This paper seeks to build on previous work using spark calorimetry that has been conducted by this lab, with a similar experimental setup and equipment [9, 10, 11] and upon the findings in the existing literature, as briefly discussed above. One of our previous studies looked at breakdown voltage, thermal energy deposition characteristics, and electrical-tothermal energy conversion efficiency trends for pressures from 1 to 24 bar, spark plug gap sizes of 0.30 mm to 1.5 mm, and dwell times of 2 ms to 6 ms, using a single 14 mm natural gas engine spark plug [9]. Another investigated spark discharge characteristics with varying electrode geometries to simulate differing scenarios of heat loss to the electrodes [10]. This included a standard plug, a spark plug with electrodes that had been shaven down to a fine point and another with electrodes that had been capped with a small piece of copper. However, those experiments showed little variation in thermal deposition characteristics among the three geometries at pressures up to 30 bar and gap sizes of 0.30 mm and 0.90 mm. Most recently, spark calorimeter experiments were conducted looking at spark plug gaps of up to 2.1 mm to represent arcs that have been stretched by a convective cross flow [11]. That study found linearly increasing thermal energy deposition with gap size and developed a correlation for energy deposition as a function of pressure and gap size. This current work differs from previous experiments in that it investigates gas compositions and spark plug geometries representative of heavy-duty natural gas engines. Our previous studies were all done in nitrogen and focused on standard 14 mm J-gap style spark plugs, whereas this present paper focuses on both noncombusting and combusting gas mixtures, as well as two different 18 mm spark plug electrode geometries. As mentioned above, the present study is motivated by the stringent demands that current and future heavy-duty natural gas engines are placing, and will place, on spark ignition systems. The higher boost and load conditions can result in spark electrode wear rates that significantly exceed those of more familiar lightduty gasoline engines in cars and light-trucks. This is an issue that can lead to significant maintenance costs, both in terms of maintenance frequency and the high cost of specialized spark plugs and ignition system components. Pertinent to this application we are examining spark plugs specifically designed for this type of heavy-duty engine which may operate with high dilution, further increasing ignition system demands.

In the present study, the discharge characteristics of an inductive spark ignition system were studied with varying gas compositions and spark plug geometries using a spark calorimeter and a constant volume optical vessel. The current, gap-voltage, and electrical and thermal energy deposition in the gap were measured for inert gases using a spark plug calorimeter for pressures up to 28 bar. The current and gap-voltage

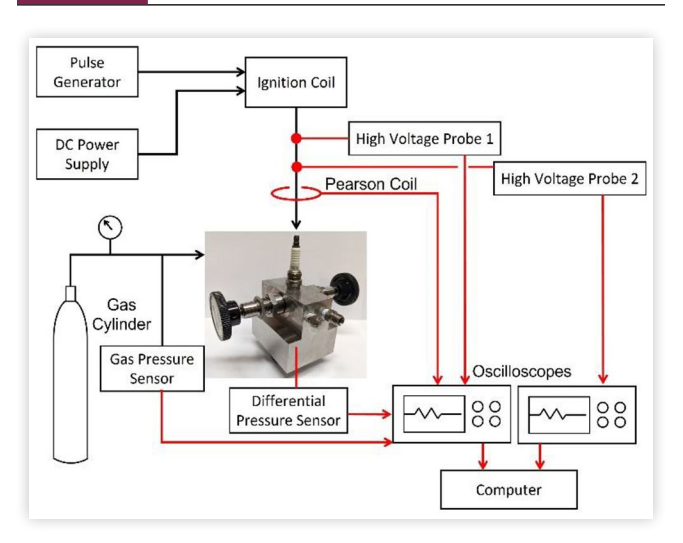
characteristics were studied for the combustible gas mixture of air and methane in a constant volume combustion chamber. The objective of the present research was to measure the effects of gas composition on spark breakdown voltage and on the thermal energy deposition to the gases near the spark gap for conditions representative of new-generation stoichiometric heavy-duty natural gas engines. These engines may be expected to operate at high bmep and with high levels of EGR dilution. All of the measurements were made under quiescent conditions so thermal energy deposition measurements did not account for arc stretch, which can be expected in an engine if there are high velocities in the gap during ignition.

# **Experimental Setup**

The setup used for this experimental study is summarized below; more details are available [11]. A calorimeter was used for non-combusting gases and gas mixtures to measure the conversion efficiency of electrical energy delivered to the gap to thermal energy deposited in the gas, as well as spark gap breakdown voltages. The calorimeter was machined from stainless steel to house a 14 mm spark plug. Since this study investigated 18 mm spark plugs, a stainless-steel adapter was created and fitted to the calorimeter. The adapter also housed a small piece of steel wool in the passage within the pressure (test) chamber of the calorimeter which was found to reduce the amplitude of the oscillations in the differential pressure signal caused by acoustic waves inside the chamber. Two valves separated the pressure chamber from the reference chamber and also allowed the inflow and outflow of gases from the pressure chamber. Between the two chambers was an Endevco 8510B-5 piezoresistive differential pressure transducer, which was rated for differential pressures up to 5 psig. This was used for measuring the very small pressure rises in the pressure chamber of the calorimeter due to the energy deposition of the spark. Six different gases or gas mixtures were investigated. This included pure gases and gas mixtures that included nitrogen as a surrogate for air, mixed with what would be a stoichiometric amount of methane. The gases included pure nitrogen, stoichiometric nitrogen and methane, stoichiometric nitrogen and methane diluted with 30% carbon dioxide, pure air and a stoichiometric methane/air mixture. The latter could not be evaluated in the calorimeter, however.

A schematic of the calorimeter experimental setup is shown in Figure 1. A pulse generator and DC power supply were connected to the ignition coil that led to the spark plug seated in the calorimeter. The ignition coil was connected to two separate high voltage probes (Tektronix Model P6015A), which were used on two different oscilloscopes set for two different time scales. A four-channel Tektronix 100 MHz oscilloscope was set to a large time scale (320ns/3 MHz) for measuring data over the duration of the discharge. This oscilloscope was also connected to a Pearson Model 110 current sensor and the calorimeter pressure transducer. The second, 2-channel Siglent 100 MHz oscilloscope was set to a very small time scale (10 ns/100 MHz) and connected to a high voltage probe for measuring breakdown voltage. It was also connected to a 500 psig Omega pressure sensor inserted in the gas supply

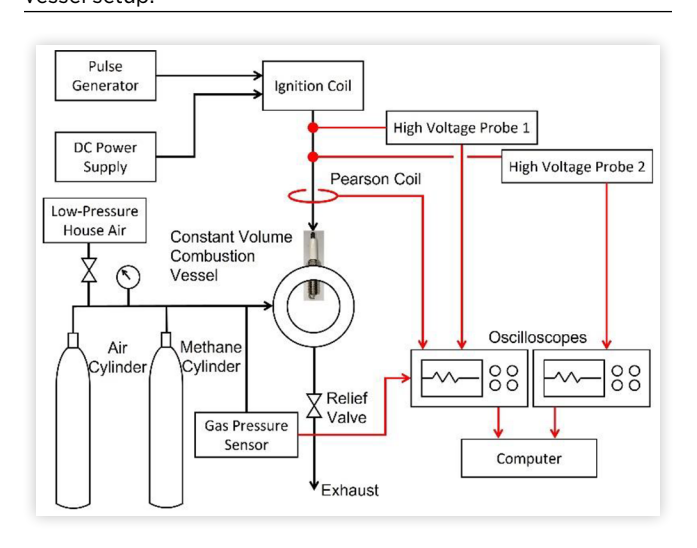
#### FIGURE 1 Schematic of calorimeter setup.



line, used to measure the pressure of gas flowing into the calorimeter. Pressures of up to 28 bar were considered for the calorimeter measurements. Both oscilloscopes fed into a computer for processing the data.

Along with the calorimeter, a constant volume combustion vessel was used for measuring the spark discharge characteristics of stoichiometric air and methane mixtures. A schematic of this setup is shown in Figure 2. The ignition coil setup remained unchanged from the calorimeter. Prior to pressurizing the combustion chamber, a supply line of compressed air at a pressure of 8 bar was used to purge the vessel. Methane was then used first to pressurize the chamber to the required partial pressure before air from a compressed air cylinder was used to bring the chamber pressure up to its final pressure, which reached 30 bar at the maximum pressure conditions tested. The high velocities of the entering gases promoted turbulent mixing and homogeneous mixtures. After combustion, a ball valve was opened to allow the pressure and exhaust gases to exit the chamber. The low-pressure air supply was then flushed through the chamber for about 2 minutes to

**FIGURE 2** Schematic of the constant volume combustion vessel setup.



remove any residual exhaust. The same voltage and current data were recorded from the oscilloscopes as from the calorimeter measurements except for the differential pressure measurements which were not applicable to the constant volume combustion vessel.

The two spark plugs considered in this study are shown in Figure 3. Both are 18 mm natural gas engine spark plugs with a gap of 0.30 mm. Figure 3a shows the standard J-gap plug used for the experiments, which had a measured internal resistance of 6.25 kOhms. Figure 3b is a plug featuring a circular center electrode surrounded by 4 ground straps, with a measured internal resistance of 6.1 kOhms. The 4-ground strap spark plugs are of interest because they have a durability advantage over J-gap sparkplugs. With 4 ground electrodes and a larger diameter center electrode there is more surface area for wear to occur before the minimum gap distance between anode and cathode increases which will lead to higher breakdown voltages and eventual failure.

#### **Results**

### **Breakdown Voltage**

Experimental measurements of breakdown voltage were recorded on a separate oscilloscope to resolve the small time scales over which the event occurs. Figure 4 shows the time scale resolutions necessary to accurately determine breakdown voltage. The dashed black line at the time of 0 s represents the data point taken as the breakdown voltage. At low pressures (less than 4 bar) the oscilloscope sampled at a frequency of 50 MHz, meaning data points were recorded every 20 ns. At higher pressures (4 bar and above), the oscilloscope sampled at 25 MHz, taking a measurement every 40 ns. This was considered fast enough to accurately measure breakdown voltage.

Breakdown voltage data is shown in <u>Figure 5</u> for the standard J-gap plug (<u>Fig. 5a</u>) and the spark plug with 4 ground straps (<u>Fig. 5b</u>). Each data point on the plots represents 40 individual measurements, taken in two trials of 20 measurements. The lone exception is the combusting air and methane

FIGURE 3 18 mm spark plugs used for the experiments with (a) a J-gap electrode geometry and (b) a 4-ground strap geometry

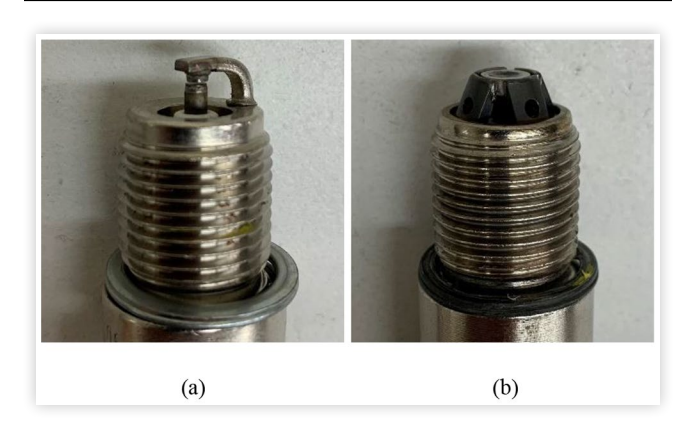
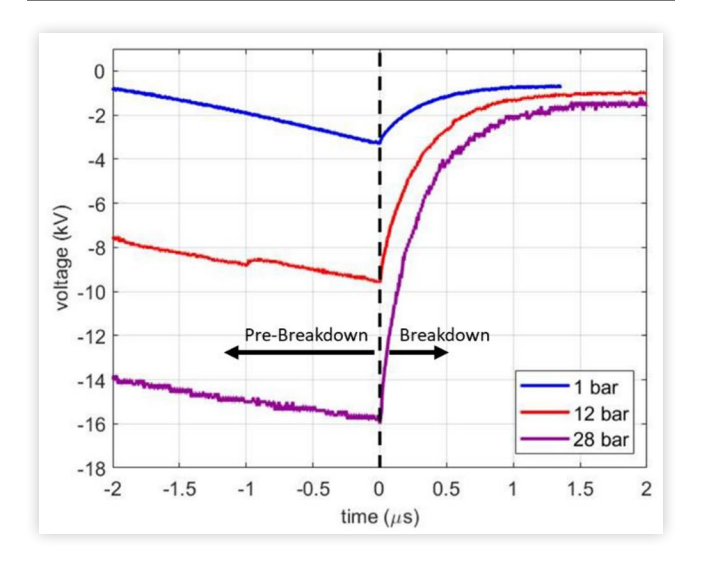


**FIGURE 4** Small time scale resolution of breakdown voltage measurements



mixture, which is only an average of 10 data points. This was due to the much larger time requirement for each sparking event, as the combustion vessel needed to be fully evacuated and extensively purged between each event to ensure minimal exhaust remained.

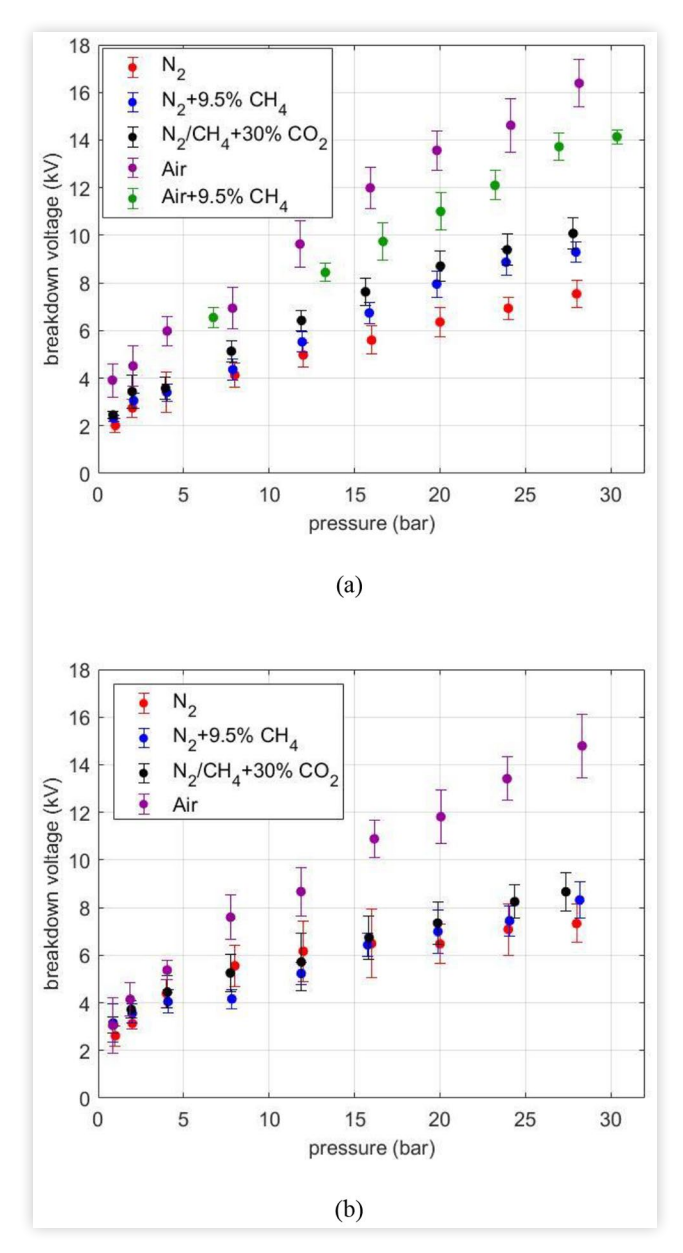
As expected, breakdown voltage increases linearly at lower pressures for both plugs, following Paschen's Law [2]. However, as also shown by Huang [4], the rate of increase of breakdown voltage begins to decline at higher pressures (above 10 bar). This trend is also significantly more noticeable for the 4-ground strap plug, which has slightly lower breakdown voltages in general when compared to the J-gap plug. This may be due to a slightly smaller gap in the 4-ground strap plug. Since the gap shape is round, it was difficult to accurately measure the gap size to within one-hundredth of a millimeter with a feeler gauge.

The breakdown voltage in air was up to 100% greater than that of nitrogen for both plugs. This suggests that nitrogen may not be representative of the discharge characteristics for pure air, or as a surrogate for air mixed with fuels that are to represent combustible gas mixtures when combustible environments are not possible. Another observation was the increased breakdown voltage with the addition of methane to nitrogen. This was more significant in the data from the J-gap plug and was as large as a 30% increase. However, the addition of methane to air had the opposite effect, reducing breakdown voltage by about 15% at high pressures. Negligible change was found from the addition of  $\mathrm{CO}_2$  to the nitrogen and methane mixture.

# **Energy Delivery/Deposition**

The electrical discharge characteristics of the spark plugs were derived from their current and voltage behavior. <u>Figure 6</u> shows examples of the current and gap voltage histories for individual shots for the J-gap spark plug and are representative of those collected. The voltages were measured at the top of each spark plug. The gap voltage, as shown, was determined

**FIGURE 5** Breakdown voltage results for (a) the J-gap plug and (b) the 4-ground strap plug at different pressures and in different gas compositions

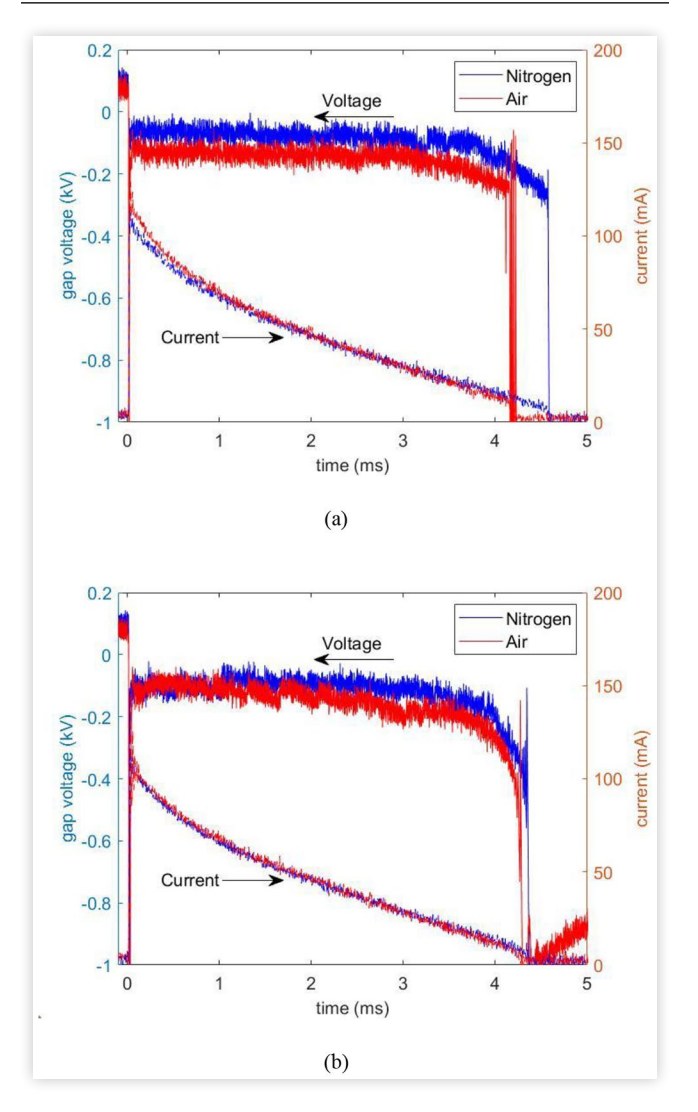


by subtracting the voltage drop across the internal resistance of the plug, which was equal to the product of the current and the internal resistance.

The initial current immediately following breakdown was approximately 100 mA for all cases and did not vary with pressure, gas mixture composition, or plug type. The follow-on gap voltages shown in Fig. 6 are for arc-type discharges and remain relatively flat over most of the discharge duration. Little difference is seen for both the current and follow-on voltage between pure air and pure nitrogen, however, the follow-on voltage was statistically greater for the air.

The following figures show the experimental results quantifying the discharge characteristics of the two spark plugs in the various quiescent gas compositions. <u>Figure 7</u> shows the follow-on voltages of the two plugs as a function of pressure.

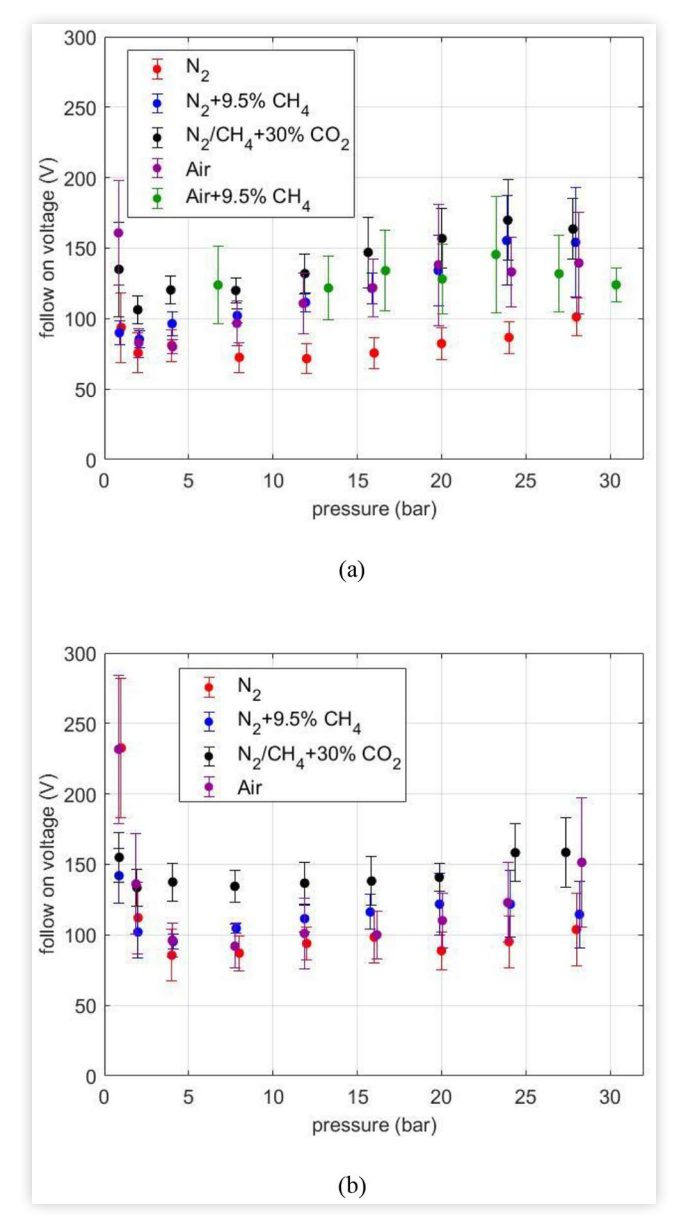
**FIGURE 6** Single-shot gap voltage and current traces for nitrogen and air for the J-gap plug at (a) 8 bar pressure and (b) 28 bar pressure.



This was determined as the average gap voltage following the breakdown event. Discharges were mainly of the glow type at atmospheric pressure but transitioned to mainly arc for pressures of 4 bar and above. The follow-on voltage data of Fig. 7 is more scattered at the lower pressures because at those low pressures the discharges could be a combination of glow and arc type discharges, while only arc type discharges were observed at higher pressures. Voltages generally increased gradually with pressure once the discharges were of the arc type, but the pressure dependence was not strong. The follow-on voltages were found to be strongly dependent on gas composition, varying by between 50% and 100%, with values for pure nitrogen being the lowest. An interesting observation was that the mixture with carbon-dioxide had the greatest average follow-on voltages.

The follow-on voltages were in the same range for the two different gap types. Follow-on voltages are of importance as these values directly correlate to the electrical energy delivered to the spark gap.

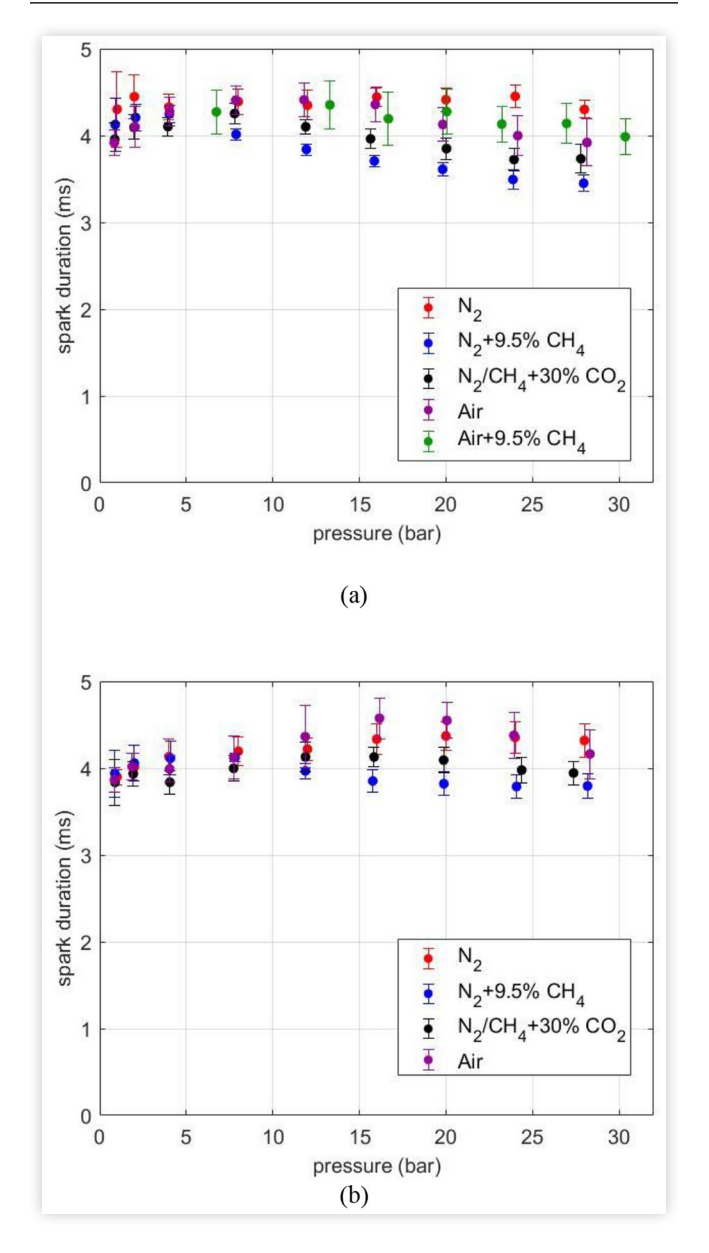
**FIGURE 7** Follow-on voltages for (a) the J-gap plug and (b) the 4-ground strap plug at different pressures and in different gas compositions



Because the current immediately following breakdown was approximately 100 mA for all conditions, the other factor in determining electrical energy delivered to the spark gap is the spark discharge duration. These data are shown in Figure 8. Typically, the spark duration decreases with increasing pressures above 8 bar [10, 11] but for the relatively small gap distance of 0.3 mm examined here, this was not the case. Here, the spark durations were nearly independent of pressure. For the 4-ground strap plug, however, discharge duration increased slightly until pressures of around 20 bar in most gas compositions.

Data for electrical energy delivered to the spark gap are shown in <u>Figure 9</u>. This was found as the integral of the gap voltage multiplied by the measured current. These plots tend to resemble those of the follow-on voltages. After the glow-type discharges near atmospheric pressure, electrical energy

**FIGURE 8** Spark discharge duration for (a) the J-gap plug and (b) the 4-ground strap plug at different pressures and in different gas compositions

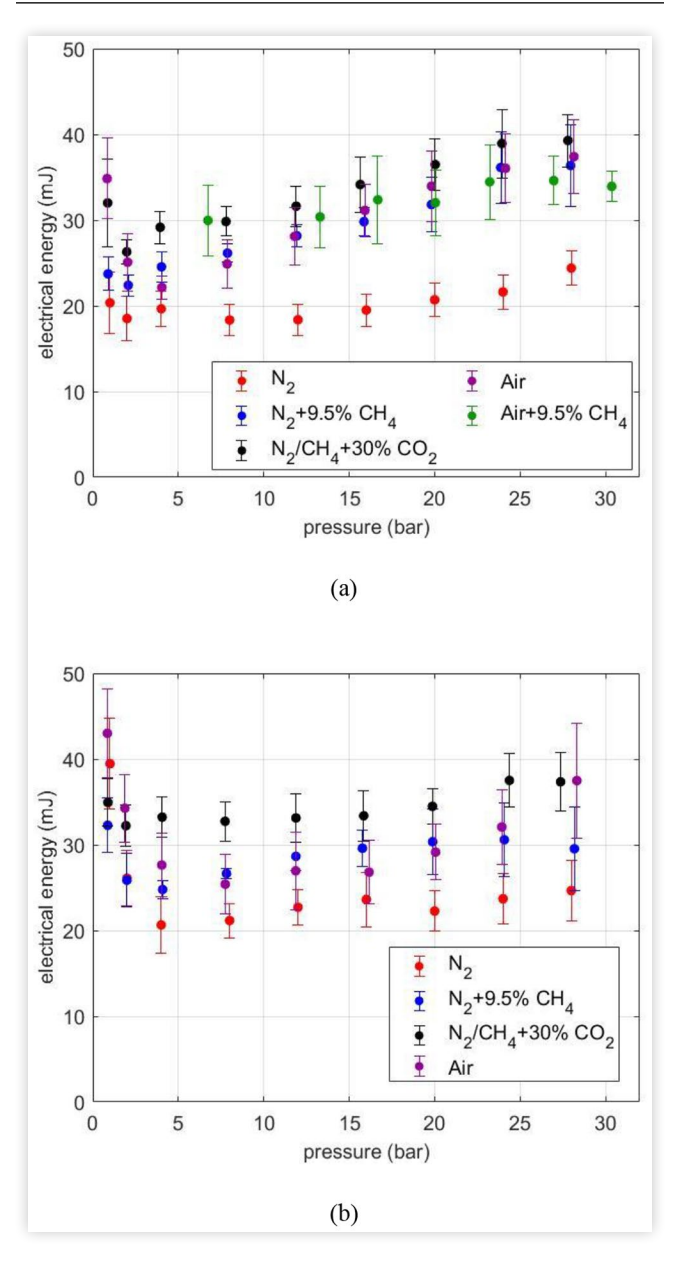


delivery increases with pressure. Nitrogen consistently had the lowest energy delivery of all the gas compositions due to its lowest voltages. The mixture of nitrogen, methane, and carbon dioxide generally had the greatest electrical energy delivery to the gap.

It is interesting that using nitrogen instead of air had a large effect on breakdown voltage, both for the pure gases and mixtures with methane; however, there was little difference between the two for follow-on voltages or electrical energy delivery to the gap. Electrical energy delivered to the gap tended to lie in the range of 20 - 40 mJ, compared with approximately 120 mJ of energy stored in the secondary side of the coil.

Using the pressure rise measurements from the calorimeter, the thermal energy deposited by the spark into the gas was calculated using equation 1 [11].

FIGURE 9 Electrical energy delivered to the spark gap for (a) the J-gap plug and (b) the 4-ground strap plug at different pressures and in different gas compositions. The higher delivered electrical energies observed in the figure at 1 and 2 bar pressures were associated with the primarily glow discharges at these pressures and follow from the observation that the sustaining glow voltages are higher than those of arc discharges.



$$E_{therm} = \frac{V}{\gamma - 1} \Delta P \tag{1}$$

In this equation, V is the volume of the chamber, measured to be 4.5E-6 m³ by filling the chamber using a water pipette,  $\Delta P$  is the measured maximum pressure rise, and  $\gamma$  is the ratio of specific heats for the given gas composition. Air/methane mixtures could not be studied since only inert gases can be used in the calorimeter.

**FIGURE 10** Raw pressure signals from the calorimeter used to determine thermal energy deposition to the gas, (a) J-gap plug, (b) 4-ground strap plug.

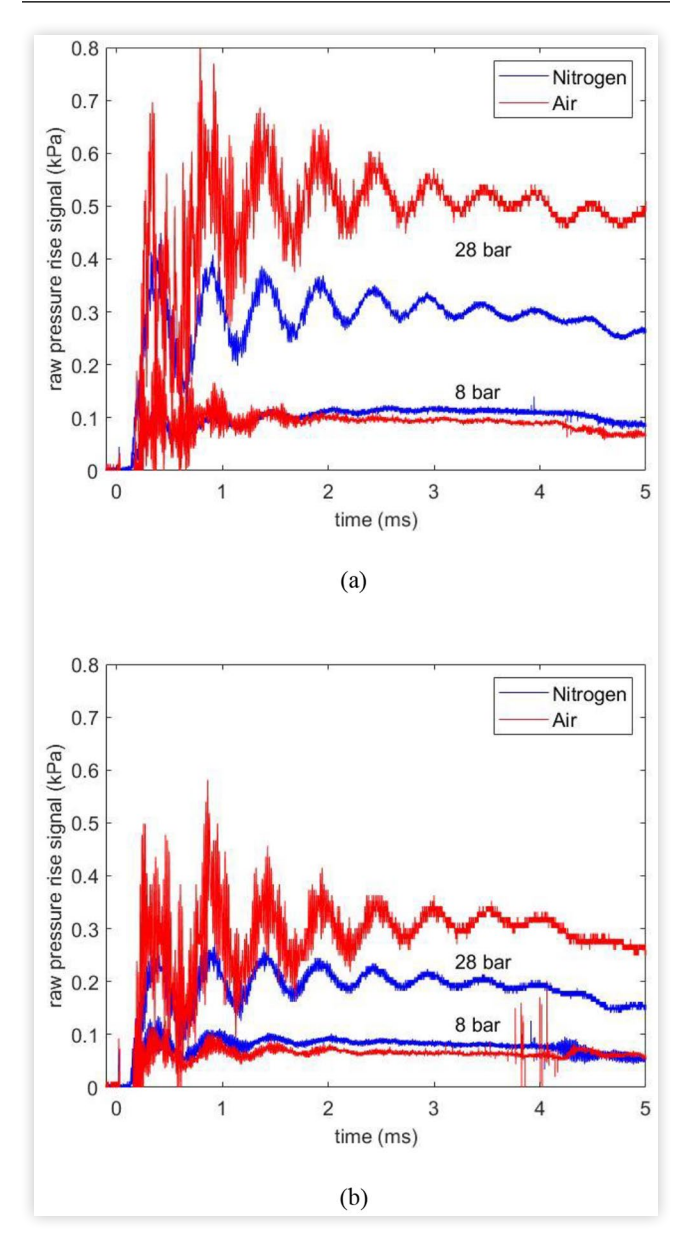
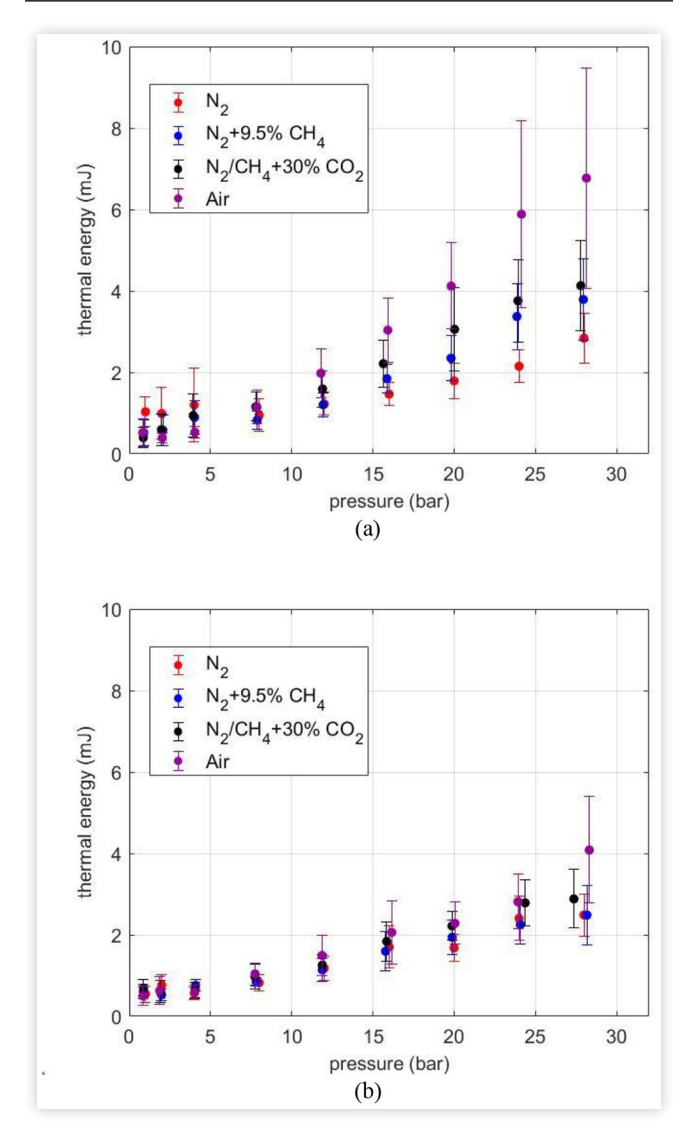


Figure 10 shows examples of raw pressure signal measurements from the calorimeter used to calculate the thermal energy deposition to the gas. The plots compare individual realizations for air and nitrogen for the J-gap plug (Fig. 10a) and for the 4-ground strap plug. Each raw data signal was curve fit and the maximum pressure was used to derive the thermal energy deposition. The minimal drop in pressure over the measurement interval illustrates the minor effect of heat loss from the gas to electrode surfaces over that period. The figures also show the considerably higher pressure rise for the J-gap plug and for air relative to nitrogen at the higher pressures. While the pressure rises were consistently higher in air than nitrogen at higher pressures (e.g., 28 bar), the observed pressures rises were similar at lower pressures (e.g., 8 bar), for which the pressure rise might be higher or lower for either gas, as it varied from shot-to-shot.

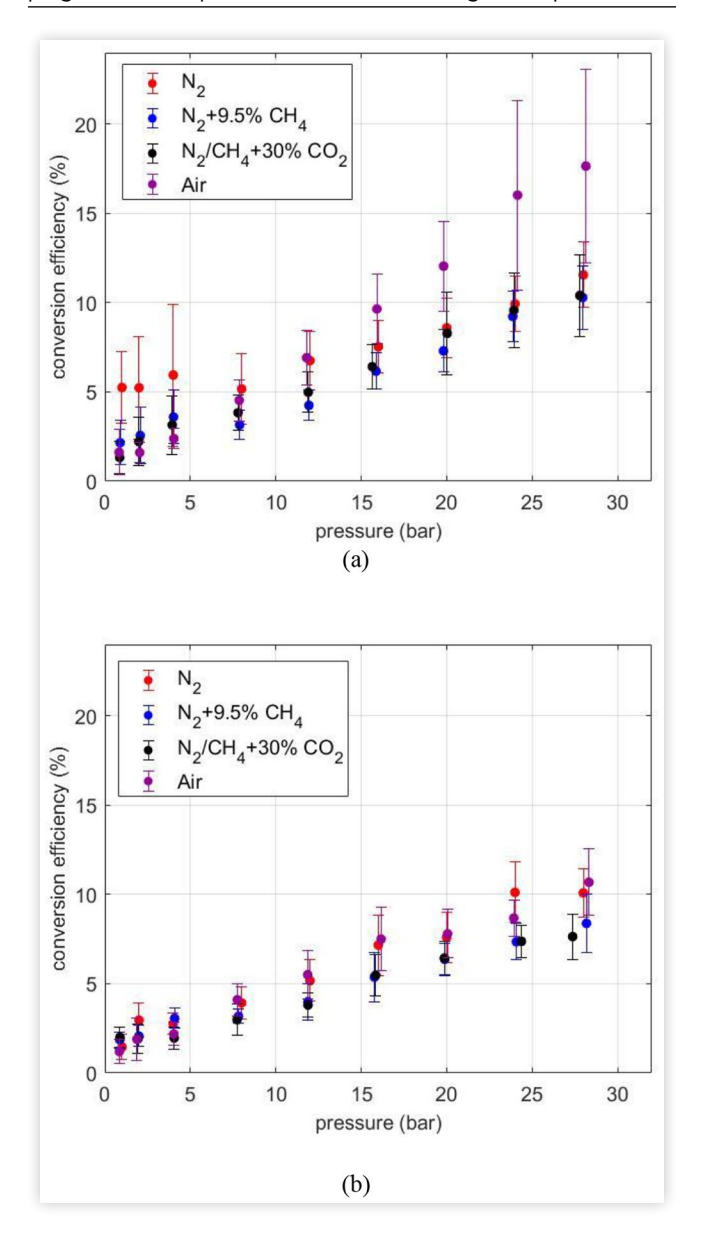
FIGURE 11 Thermal energy deposited in the gas for (a) the J-gap plug and (b) the 4-ground strap plug at different pressures and in different gas compositions



The thermal energy deposition measurements are shown in Figure 11.

The thermal energy deposition was significantly different between the two plug geometries but consistently increase with pressure. For the standard J-gap style plug, air and nitrogen represent the two extremes of energy deposition, with the spark depositing the most energy in air and the least in nitrogen. At the higher pressures, the energy deposition in air was as much as three times higher than in pure nitrogen. The reason for this difference is not clear. Oxygen and nitrogen have similar thermal conductivities and thermal diffusivities so it is unlikely that the differences in thermal energy deposition are due to differences in heat diffusion rates to the electrodes. Nitrogen, N2, has a significantly higher ionization energy (15.6 eV) than  $O_2$  (12.2 eV) [12]; the relative ease of ionizing O<sub>2</sub> may enhance energy absorption within the gas. The addition of carbon dioxide also tended to slightly increase the energy deposition when compared to the nitrogen and methane mixture. Interestingly, for the 4-ground strap plug,

**FIGURE 12** Electrical-to-thermal energy conversion efficiency for (a) the J-gap plug and (b) the 4-ground strap plug at different pressures and in different gas compositions



gas composition had a negligible effect on thermal deposition. These values were generally lower than for the J-gap plug, most notably in the air case. Thermal energy values were up to 50% lower for the 4-ground strap plug. This was attributed to the larger surface area and annular-shaped gap of the plug, resulting in greater heat losses, and thus, lower thermal energy deposition.

Energy conversion efficiency was calculated as the ratio of thermal energy deposited in the gas to electrically energy delivered to the gap. The remaining energy delivered to the gap that does not go to increasing the thermal energy deposition is lost to heat transfer and contributes to spark plug erosion. [10] The conversion efficiency measurements are shown in Figure 12 as a function of pressure. These plots follow similar trends to those of Figure 11. For the J-gap style plug, the air case shows a considerable increase in energy conversion

over the other cases. The nitrogen case and its mixtures present negligible differences amongst each other. The 4-ground strap plug again shows negligible differences between the conversion efficiency in air or nitrogen. However, conversion efficiency in nitrogen and its mixtures are very similar between the two spark plug geometries.

# **Summary and Conclusions**

Two different 18 mm diameter natural gas engine spark plugs having different electrode geometries were characterized for the electrical and thermal discharge characteristics over a range of pressures up to 30 bar and for different gas compositions for a fixed gap distance of 0.3 mm. This gap was chosen as it is used with certain current heavy-duty high BMEP natural gas engines. While most of the measurements were made with inert gases/mixtures using a spark plug calorimeter, some measurements included combustible stoichiometric air/methane mixtures using a constant volume combustion chamber. Notable observations include the following.

- 1. It was found that while the electrical energy delivered to the J-gap plug and the 4-ground electrode plug were similar, the thermal energy delivered to the gas was up to 50% lower for the 4-ground strap plug.
- 2. The thermal energy delivered to the gas was strongly dependent on gas composition, especially for the J-gap plug. The thermal energy delivered to the gap was more than twice as great for pure air relative to pure  $N_2$  in the case of the J-gap plug.
- 3. The breakdown voltages were found to be strongly dependent on gas composition. Air was found to give breakdown voltages up to twice as large as those found for pure nitrogen, presumably due to the lower ionization energy of  $O_2$  relative to  $N_2$ . The addition of methane to nitrogen increased breakdown voltage by up to 20% for pressures of 12 bar and greater for the J-gap plug; for the 4-ground electrode plug the increases with added methane were small but showed a consistent increase.
- 4. At the relatively small gap size investigated, spark duration was little affected by both gas composition and pressure.
- 5. Electrical energy delivered to the gap increased with pressure for the J-gap plug, but was relatively insensitive to pressure for the 4-electrode plug. It was also significantly lower for pure N<sub>2</sub> than for the other gases/mixtures, where the other gases/mixtures were similar in their electrical energy delivered to the gap.
- 6. Overall conversion efficiencies of electrical energy to thermal energy in the gap were low for the small gap size studied. They increase strongly with increasing pressure ranging from as low as 1% at one bar to as high as 15% for air at 28 bar. The conversion efficiencies were not strongly dependent on gas composition but were highest for air in the arc regime at higher pressures and were highest for N<sub>2</sub> in the glow regime at low pressures, near atmospheric.

#### References

- 1. Cho, H.M. and He, B.-Q., "Spark Ignition Natural Gas Engines A Review," *Energy Convers Manag* 48, no. 2 (2007): 608e18.
- Meek, N.F., Electrical Breakdown of Gases, (London, UK: Oxford at the Clarendon Press, 1953).
- 3. Pashley, N., Stone, R., and Roberts, G., "Ignition System Measurement Techniques and Correlations for Breakdown and Arc Voltages and Currents," SAE Technical Paper 2000-01-0245, 2000, https://doi.org/10.4271/2000-01-0245.
- 4. Huang, S. et al., J. Phys. D: Appl. Phys. 53 (2020): 045501.
- Roth, W., Guest, P.G., Elbe, G., and Lewis, B., "Heat Generation by Electric Sparks and Rate of Heat Loss to the Spark Electrodes," *J. Chem. Phys.* 19 (1951): 1530-1535.
- 6. Teets, R. and Sell, J., "Calorimetry of Ignition Sparks," SAE Technical Paper 880204, 1988, https://doi.org/10.4271/880204.
- Abidin, Z. and Chadwell, C., "Parametric Study and Secondary Circuit Model Calibration Using Spark Calorimeter Testing," SAE Technical Paper 2015-01-0778, 2015, https://doi.org/10.4271/2015-01-0778.
- 8. Franke, A. and Reinmann, R., "Calorimetric Characterization of Commercial Ignition Systems," SAE Technical Paper 2000-01-0548, 2000, <a href="https://doi.org/10.4271/2000-01-0548">https://doi.org/10.4271/2000-01-0548</a>.
- Kim, K., Hall, M.J., Wilson, P.S., and Matthews, R.D., "Arc-Phase Spark Plug Energy Deposition Characteristics
   Measured Using a Spark Plug Calorimeter Based on
   Differential Pressure Measurement," *Energies* 13 (2020):
   3550, doi:10.3390/en13143550.

- 10. Kim, K., Tambasco, C., Hall, M., and Matthews, R., "Experimental and Modeling Study of Spark Plug Electrode Heat Transfer and Thermal Energy Deposition," SAE Technical Paper 2021-01-0480, 2021, <a href="https://doi.org/10.4271/2021-01-0480">https://doi.org/10.4271/2021-01-0480</a>.
- Tambasco, C., Li, D., Hall, M., and Matthews, R., "Spark Ignition Discharge Characteristics under Quiescent Conditions and with Convective Flows," SAE Technical Paper 2021-01-1157, 2021, https://doi.org/10.4271/2021-01-1157.
- 12. Fridman, A. and Kennedy, L.A., *Plasma Physics and Engineering*, (New York: Taylor & Francis, 2004).

#### **Contact Information**

Prof. Matthew J. Hall
mjhall@mail.utexas.edu
The University of Texas at Austin
Department of Mechanical Engineering
204 E. Dean Keeton St. C2200
Austin, TX 78712

### **Acknowledgments**

This project was made possible through funding provided by Cummins Inc. through the University of Texas at Austin's site of the NSF Center for Efficient Vehicles and Sustainable Transportation Systems (EVSTS). The authors wish to express their gratitude to Sachin Joshi, Daniel J. O'Connor and Douglas L. Sprunger of Cummins Inc. for many helpful discussions.